ARMA 11-442

Modeling unstable rock failure during a uniaxial compressive strength test

Kias, E. M. C.
Gu, R., Garvey, R., and Ozbay, U.
Colorado School of Mines, Golden, Colorado, U.S.A.

This paper was prepared for presentation at the 45th US Rock Mechanics / Geomechanics Symposium held in San Francisco, CA, June 26–29, 2011.

ABSTRACT: In this study we investigate unstable compressive failure of rock using numerical modeling. An unconfined compression test with variable platen stiffness is modeled using three different finite difference based numerical models: a continuum model (FLAC3D), a distinct element model comprised of blocks with interfacing joints (3DEC), and a distinct element model comprised of bonded spheres (PFC3D). In each case we show that unstable failure can be modeled according to the theory that instability occurs when potential energy stored within a relatively soft loading system is quickly transferred to the loaded rock as it fails, rescinding its ability to withstand load. Instability is detected in each model when a period of rapid platen rebound causes a sudden reduction of strength in the sample. Whereas during stable failure, the post-peak modulus of the failing specimen is observed to follow the unloading curve of the characterisitc material in a stable softening mode. Each model type reproduces similar behavior in both stable and unstable failure.

1. INTRODUCTION

Unstable rock failures in deep mining and tunneling conditions may result in rockburst events that can cause serious harm to workers and equipment. A good understanding of unstable rock failure has been developed through decades of extensive laboratory testing. However, the theoretical background acquired has not been extended into in-situ conditions to a satisfactory degree of certainty or usefulness. Current numerical modeling techniques offer potential for furthering available knowledge on the fundamental mechanisms of unstable failures. Successful development of such modeling techniques for the analysis of rockbursts may lead to safer designs for mining and tunneling operations.

Fig. 1 shows a version of the classical diagram from Cook's [4] presentation of the stable and unstable failure conditions that can occur during laboratory uniaxial compressive strength (UCS) testing of a rock specimen. The stress-strain curve shown with a solid line represents the specimen's characteristic behavior, which can only be obtained under stable loading conditions with a sufficiently stiff or servo-controlled loading machine [5]. Stability of loading in the post-peak region is not a given but is determined by the relative stiffnesses of the specimen's characteristic softening behavior and the testing machine. Stable failure occurs as long as the softening slope is shallower than the slope of the machine load line, as in the case of the dashed line, "Stiff Loading System" in Fig. 1. If the machine load line is shallower than the softening slope, i.e. the case of "Soft Loading System" line in the same figure, the specimen cannot meet the machine's load demand and unstable failure occurs [6]. The intensity of such failure is determined by the difference between the material

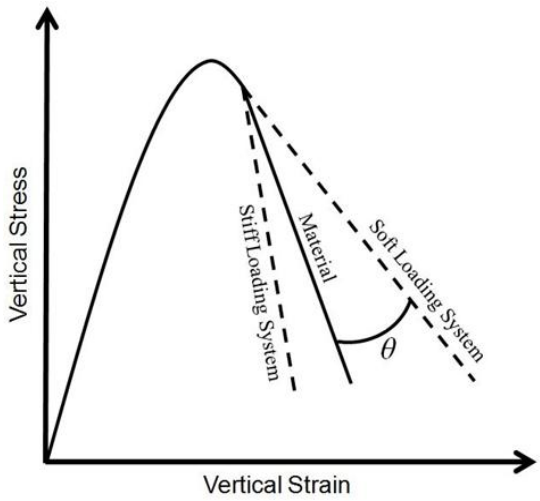

Fig. 1. Classic stability theory of UCS testing

post-peak stiffness and the stiffness of the loading system in other words, by the angle θ in Fig. 1.

The work described here is an initial step of evaluating three numerical modeling codes, namely FLAC3D [1], 3DEC [2] and PFC3D [3], for their ability in modeling stable and unstable failure during a UCS test. The material selected for the tests has a stress-strain behavior similar to that shown in Fig. 1. This behavior is obtained from a series of calibration simulations for each model. The calibrated specimen is placed between two cylindrical steel platens that represent the testing machine. The shape, size, and properties of the specimen are kept the same for all tests. The loading system stiffness is varied by changing the elastic modulus of the steel platens. The results are presented in standardized plots specifically developed for comparison purposes.

2. GENERAL MODEL DESCRIPTION

In this study, the numerical modeling of UCS tests and the measurement methods are developed based on the failure stability concept described above. The simulated test specimen has material properties close to some of the coal seams being mined in the western United States. The failure of such coal can be defined using the Mohr-Coulomb parameters friction angle, $\varphi = 30°$, and cohesion, c = 2.4 MPa. The specimen is cylindrical in shape with a diameter of 1 m and height of 2 m placed between a pair of 1 m high 1 m diameter steel platens. The complete characteristic stress-strain curve of the specimen used in modeling exhibits strain-softening behavior after peak strength, as is shown in Fig. 2a. The load is introduced by applying constant axial displacement at the ends of the platens. The interface at the steel–specimen contact is assigned a friction angle of 15^o. The effect of loading system stiffness is then controlled by adjusting Young's modulus of the platens.

The results of the numerical modeling studies are presented in the form of stress-strain plots similar to those shown in Fig. 3 and Fig. 4. The stresses are

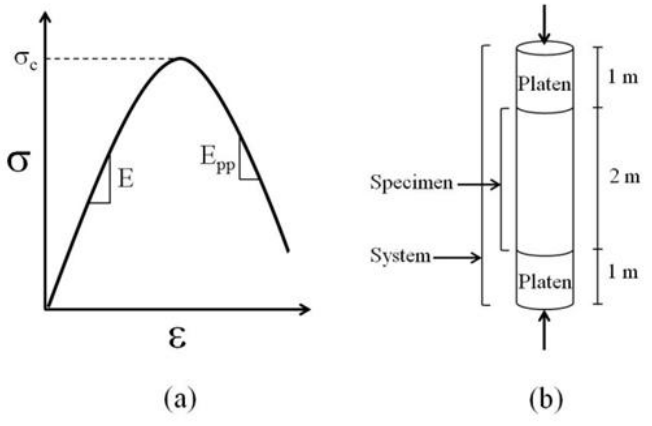

Fig. 2. Characteristic material and model configuration

plotted for two separate measurements of strain; one by considering only the specimen and the other by considering the combined specimen and platen strain. These strain measurements are referred to as "specimen" strain and "system" strain, respectively (Fig. 2b). Fig. 3 shows stable and unstable failure in terms of the specimen strain by taking L_{spec} as length. During stable failure the stress-strain curve follows the material

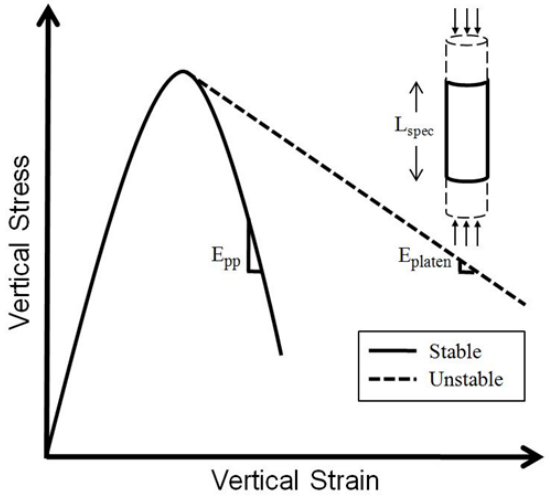

Fig. 3. Stress-strain response as measured by "specimen"

properties as indicated by the solid line. The dashed line shows unstable failure, where the totally destroyed specimen does not have a post-peak curve and the strain measured is that of platens during their elastic rebound.

Fig. 4 illustrates stable and unstable failure curves using the system strain which takes L_{sys} as length. The solid line represents stable failure in terms of system strain where the steady crushing of the material by a rigid loading system results in a post-peak slope given by the composite stiffness of the specimen and the platens. The dashed line represents unstable failure when using soft elastic platens. Here, the shift in the ascending part of the curve is due to reduced platen elastic modulus. The

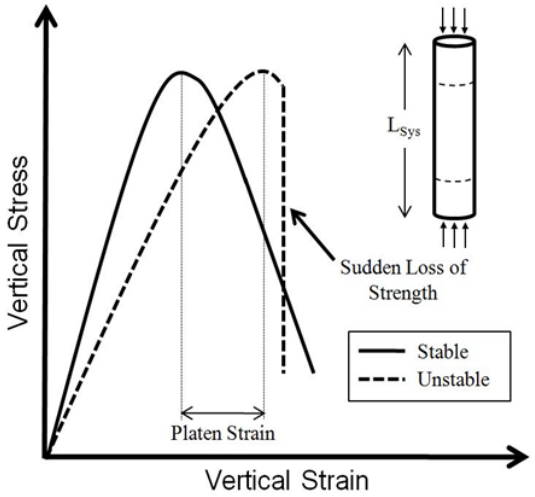

Fig. 4. Stress-strain response as measured by "system"

system strain measurement records unstable failure as almost total loss of load. The space between the peaks of the stable and unstable curves denotes the additional strain in the soft platens that rebound elastically at failure. Note the slight difference in the stable curve as compared to the specimen stable curve due to the composite stiffness of the platen and specimen system.

The model compressive strength tests were performed using three numerical models: FLAC3D, 3DEC, and PFC3D. For each model, the tests were repeated for three different platen modulus values of 100 GPa, 10 GPa, and 1.5 GPa.

3. MATERIAL CALIBRATION

A calibration process, unique to each model type, was applied for each numerical modeling method in order to generate a specimen with material properties approximating the material characteristics listed as "Target" values in Table 1. For the calibration process, the specimen of equal dimension to the final model specimen was loaded by applying constant axial displacement directly at its top and bottom surfaces. Platens of near rigid stiffness, 400 GPa, were used for the FLAC3D and 3DEC tests to preserve the effect of the installed interface while rigid walls were used in the PFC calibration. Fig. 5 shows the characteristic values of the modeled specimen curves as obtained from the three numerical models. The post-peak modulus for the models was determined as the slope of the line drawn between points on the specimen stress-strain curve at stress values found at 90% and 50% of peak stress during failure. For all models, elastic modulus and Poisson's ratio are both calculated using the origin and the point on the loading portion of the curve at 50% UCS. These values are shown in Table 1 next to the target values for the ideal material.

Table 1. Characteristic material properties

	Target	FLAC3D	3DEC	PFC3D
UCS (MPa)	7.6	7.5	7.6	7.5
E (GPa)	4.0	4.0	4.0	4.2
Epp (GPa)	-4.0	-4.0	-4.1	-5.75
ν	0.2	0.2	0.2	0.2

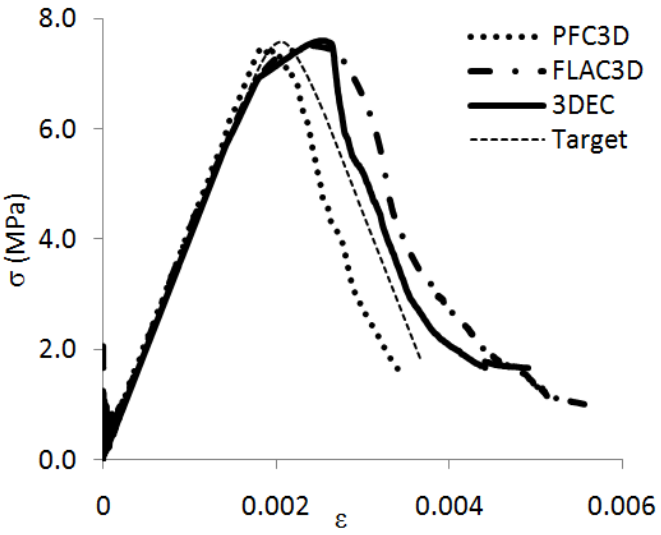

Fig. 5. Model specimen generated stress-strain curves

The model stress-strain curves shown in Fig. 5 differ from the target material in unique ways for each numerical modeling method which was employed. For example, the PFC3D curve shows small hardening, while both the FLAC3D and 3DEC models exhibit a region of hardening before the peak. Also, fluctuations in the post-peak region are a testament to the difficulties in obtaining the target value for E_{pp}. For the purpose of this study, the use of E_{pp} is generalized in the sense that its average trend is compared to the platen stiffness in concluding whether the failure is stable or unstable.

4. FLAC3D TESTS

A three-dimensional coal and platen model was constructed in FLAC3D as is shown in Fig. 6. The platens were modeled elastically and the coal was represented using the strain-softening constitutive model. Interface contact behavior of friction angle 15° is assigned between the coal and platens to simulate confinement effects at the top and bottom of the coal sample. Fig. 7 shows the calibrated strain-softening material properties for the coal specimen. Within the strain-softening model, parameters for cohesion, friction angle and dilation angle in the coal specimen are

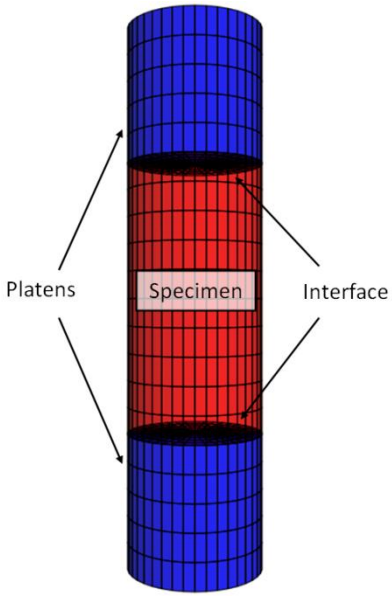

Fig. 6. FLAC3D model geometry

adjusted as the specimen plastic strain achieves pre-defined values. For example, as shown in Table 2, the third row in the cohesion section means that when the specimen plastic strain within a zone is 0.0090, the cohesion will be changed to 0.50 MPa for that zone. The calibrated set of parameters resulted in a sample material response which approximately represents the material properties listed in Table 1. However, the sample material does exhibit variations in slope in the post-peak region which will later be discussed in more detail.

Table 2. FLAC3D strain-softening parameters

Cohesion (plastic strain, MPa)	0.0000,2.41 0.0005,2.41 0.0090,0.50 0.0155,0.26 0.0160, 0.26
Friction Angle (plastic strain, degree)	0.0000,0.10 0.0001,25.0 0.0010,30.0 0.0100,30.0
Dilation Angle (plastic strain, degree)	0.0000,0.00 0.0010,15.0 0.0070,15.0 0.0120,5.00

Three UCS tests were performed with the elastic modulus of the platens being 1.5 GPa, 10 GPa, and 100 GPa. Fig. 7 shows the calibrated material behavior and the platen load lines. Axial stress within the coal specimen was monitored during the tests by averaging reaction forces across the specimen's cross-sectional area at the top and bottom of the specimen. The specimen and system responses in each of these tests are shown in Fig. 8 and Fig. 9. These two figures are analogous to Fig. 3 and Fig. 4 in showing the stress-strain behavior of the specimen and system during each UCS test.

By examining the post-peak slopes in Fig. 8 and Fig. 9, an unstable failure is identified for the 1.5 GPa case. In Fig. 8, the unstable failure manifests itself as a change in post-peak slope of the specimen stress-strain response to assume the unloading modulus of the platen. In Fig. 9, the system response curve for the 1.5 GPa test also shows instability as demonstrated by a sharp drop in the strength with little increase in system strain. The specimen and system response both identify the failure as unstable when using 1.5 GPa platens. In contrast, neither of these indicators for instability are readily observed for the 10 GPa or 100 GPa platens.

A subtle result emerges when upon further study of the stress-strain curve of the system during failure in the case of 10 GPa platens. The system curve shown in

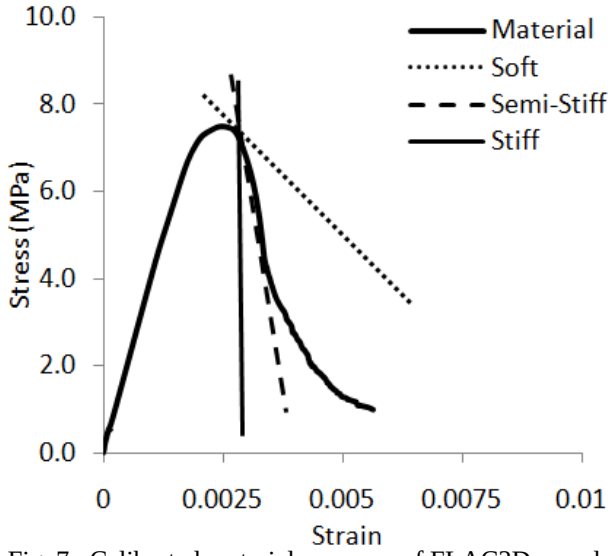

Fig. 7. Calibrated material response of FLAC3D sample. Superimposed load lines represent 1.5 GPa (Soft), 10 GPa (Semi-Stiff), and 100 GPa (Stiff) platens

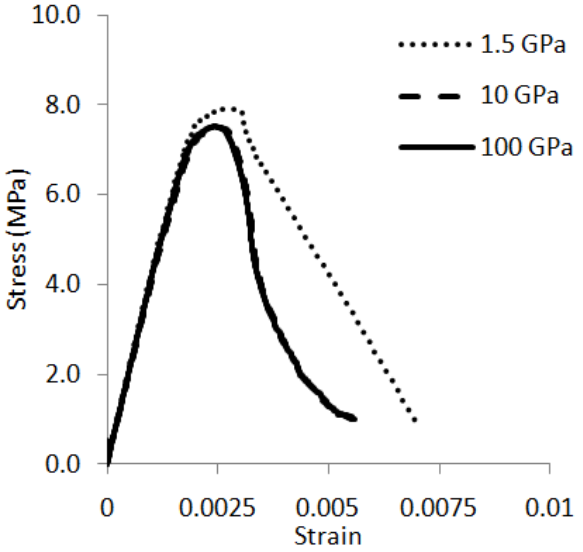

Fig. 8. FLAC3D specimen response for varying platen stiffnesses

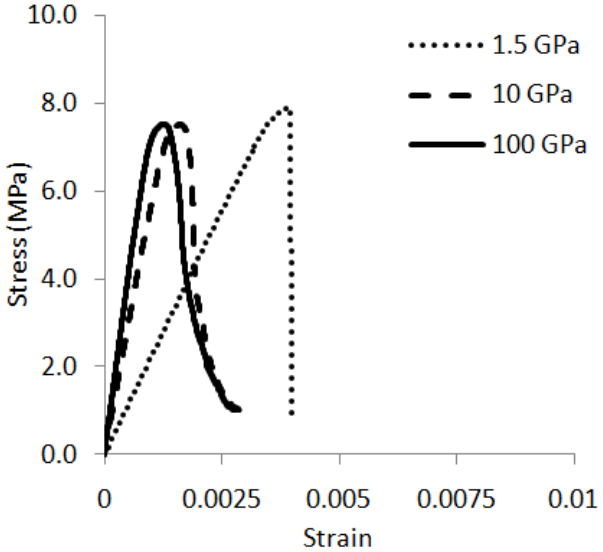

Fig. 9. FLAC3D system response for varying platen stiffnesses

Fig. 9 assumes a very steep slope of -147 GPa_at one point during the test_of the semi-stiff platens. This behavior occurs only for a brief portion of the test but is an indication of unstable failure. In order to more closely study the system's response when using 10 GPa platens, a modified loading procedure was applied to the system that included frequent pauses in the test as the specimen was failing. During each pause, the velocity boundary at the top and bottom of the platens was set to zero and the system was allowed to come to equilibrium.

Under stable loading conditions, the system would quickly come to equilibrium after each pause. For unstable loading conditions where the stiffness of the platens was less than the stiffness of the coal, the specimen would continue to fail due to platen rebound even if the total system strain increment was paused.

Fig. 10 shows the specimen stress history during the 10 GPa platen test when using the modified testing procedure. The platens were paused after every 0.1 MPa

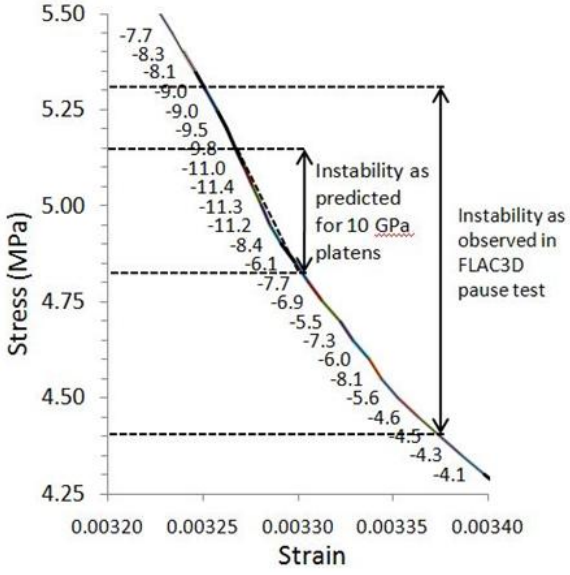

Fig. 10. Specimen stress vs. time step while using modified testing procedure with pauses during failure

drop in sample strength. As seen in the figure, a sudden drop in strength occurs in the specimen during a pause step at 5.3 MPa. The specimen continues to fail unstably until it reaches a residual strength of 4.4 MPa. At this point the system regains static equilibrium and no additional indications of instability are observed in the remainder of the test.

In order to explain this period of temporary instability in the 10 GPa platen test, the detailed post-peak behavior of the FLAC3D coal specimen was analyzed in the range of 4.2 MPa to 5.4 MPa. Results of this study are shown in Fig. 11. The local post-peak modulus is listed in GPa next to the specimen's stress-strain curve in 0.05 MPa increments of stress. It was determined that the strain-softening coal specimen was calibrated to have an

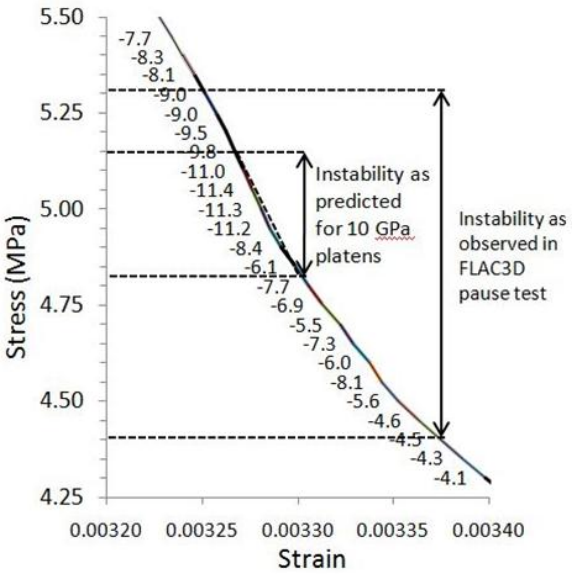

Fig. 11. Detailed material response of calibrated strain-softening coal model. Loacal post-peak moduli in GPa and recorded over 0.05 MPa increments.

average post-peak modulus of -4 GPa, however difficulties in the manual calibration process for the strain-softening model had led to a non-linear post-peak curve with local post-peak moduli as steep as -11.4 GPa. Stability theory would therefore indicate that the calibrated material response shown in Fig. 7 would indeed lead to a transient unstable failure when using the semi-stiff 10 GPa platens. The unstable failure should begin at approximately 5.15 MPa when the specimen local post-peak modulus falls below the unloading modulus of the platens. The specimen behavior should then assume the unloading modulus of the platens until a static equilibrium condition is satisfied around 4.8 MPa. Fig. 11 shows that the range of instability determined through the FLAC3D pause test is slightly greater than the range predicted by theory. The cause for this discrepancy is not immediately apparent and future work should be done to investigate temporarily unstable failures in a strain-softening numerical model. Overall, the results demonstrate that the cases of unstable, stable and temporarily unstable failures within a simulated rock specimen could be detected by FLAC3D using multiple identification methods.

5. 3DEC TESTS

The 3DEC model geometry and joint orientation is shown in Fig. 12. Three Dimensional Distinct Element Code, 3DEC, allows modeling of a discontinuous medium as an assemblage of discrete blocks. In 3DEC modeling of a UCS test, three sets of joints are embedded in the specimen: two vertical sets perpendicular to each other, and one horizontal set. The spacing is 0.4 m between horizontal joints, and 0.1 m between vertical joints. The joints are assigned as

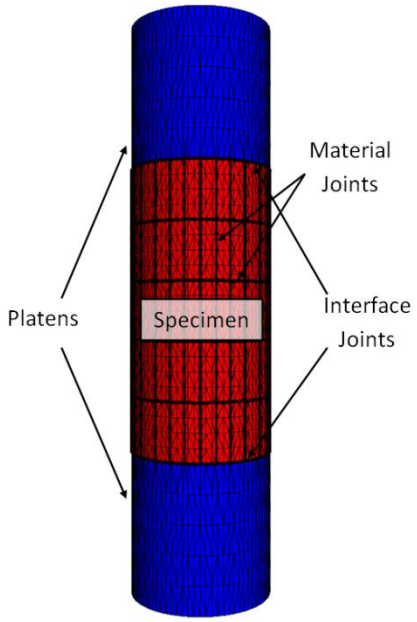

Fig. 12. 3DEC model geometry and joint orientation

Coulomb Slip model with the parameters listed in Table 3. These discontinuities roughly represent the face and butt cleats encountered in coal seam material. The blocks created by the joint sets are further discretized into zones of strain-softening material, while the platens are discretized into zones of elastic material with the properties of steel. The average length of the zone edge is 0.1 m and 0.2 m for the specimen and platens, respectively. The loading is induced by applying constant velocity of 7.5×10^{-3} m/s at both the top and bottom of the steel platens.

The characteristic material stress-strain curve after calibration in 3DEC is shown in Fig. 13. The specimen was calibrated to have similar properties as "Target" values listed in Table 1. The strain-softening parameters assigned to the zones of the specimen in the models are listed in Table 4.

Table 3. 3DEC material joint parameters

Parameter (Unit)	Value
Cohesion (MPa)	1.0
Friction Angle (Degree)	30.0
Dilation Angle (Degree)	15.0
Tensile Strength (MPa)	0.0
Normal Stiffness (GPa/m)	50.0
Shear Stiffness (GPa/m)	100.0

Table 4. 3DEC strain-softening parameters

Cohesion (plastic strain, MPa)	0.0000,2.15 0.0005,2.15 0.0272,0.12
Friction Angle (plastic strain, deg.)	0.0000,15.0 0.0001,25.0 0.0010,30.0 0.0070,30.0
Dilation Angle (plastic strain, deg.)	0.0000,0.0 0.0010,15.0 0.0070,15.0 0.0120, 5.0

The specimen stress-strain curves for different platen stiffness loading are shown in Fig. 14 and Fig. 15. The results are similar to those obtained from the FLAC3D modeling. Fig. 14 shows that for stiff loading systems (100 GPa and 10 GPa), the post-peak behavior is close to the material characteristic behavior, indicating that specimen failure took place in a stable manner. For the soft loading system (1.5 GPa), the post-peak modulus approximates that of the steel platen modulus of 1.5 GPa, implying rapid platen rebound during unstable failure as discussed in the previous sections of FLAC3D tests. The residual strength in the graph is thought to be due partly to the residual strength assigned in the strain softening model and also to block interlocking occurring within the specimen.

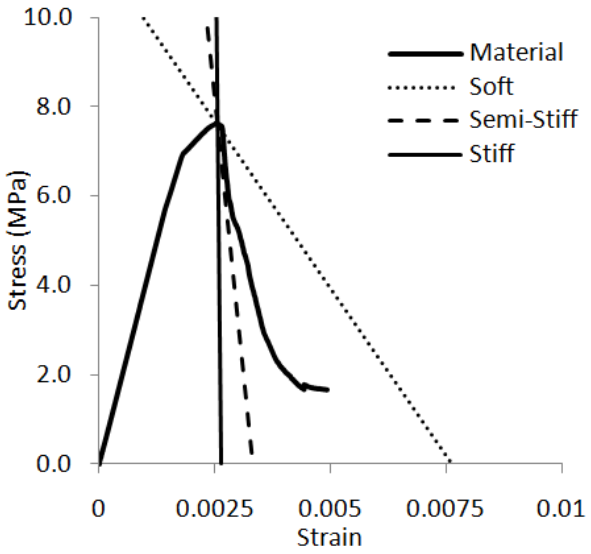

Fig. 13. Material response of 3DEC sample

The post-peak moduli of the specimen stress-strain curves for each test are shown in Table 5. In general the values in the table are in accord with the previously described stable/unstable failure conditions. Values in the darker shaded region list expected and measured specimen post-peak moduli for the unstable failure, and values in the lighter shaded region list expected and measured specimen post-peak moduli for the stable failure. For the unstable failure, the measured specimen

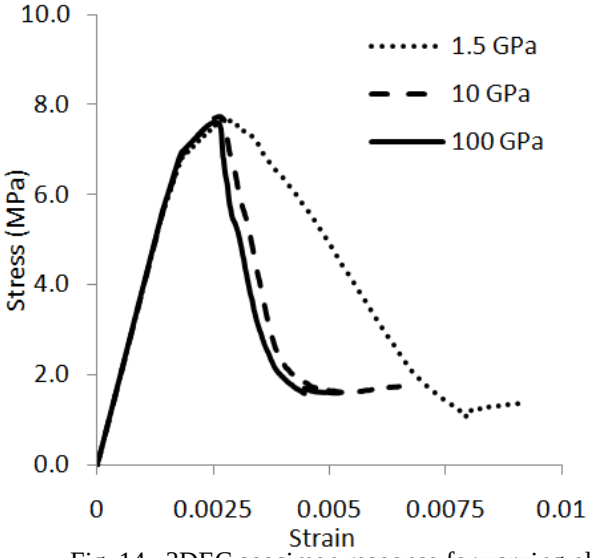

Fig. 14. 3DEC specimen response for varying platen stiffnesses

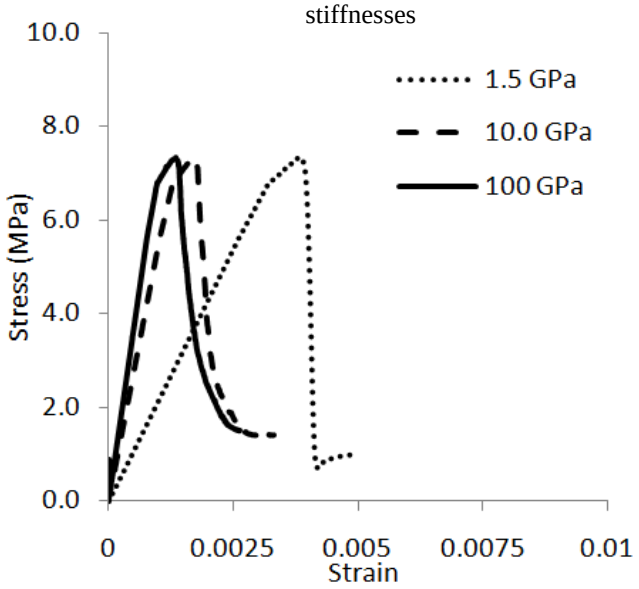

Fig. 15. 3DEC system response for varying platen stiffesses

Table 5. 3DEC test post-peak moduli

	Platen E (GPa)	Measured Specimen E_{pp} (GPa)	Material E_{pp} (GPa)
Soft	1.5	-1.5	-4.1
Semi-Stiff	10	-4.1	-4.1
Stiff	100	-4.1	-4.1

post-peak modulus matches the platen modulus and for the stable failure the measured specimen post-peak modulus matches the characteristic material post-peak modulus.

6. PFC3D TESTS

The PFC3D model specimen consists of an assemblage of discrete spherical particles that are bonded together with cylindrical beams in order to simulate a solid material. The PFC3D model geometry is shown in Fig. 16. Table 6 shows the micro parameters used to generate an in-situ coal specimen similar to the material described by Table 1. The micro-parameters shown in Table 6 were established using the iterative calibration procedure described in [7]. The specimen is comprised of particles with density, ρ, and a uniform particle size distribution determined by the ratio of minimum particle diameter, D_{min}, and maximum particle diameter, D_{max}, where D_{min} = 23 *mm*. The friction coefficient between

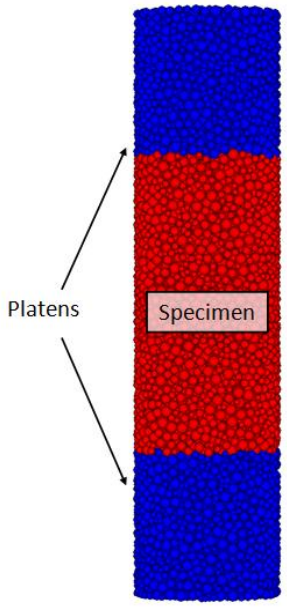

Fig. 16. PFC3D model geometry

the balls is denoted by μ. Stiffness of the particles and bonds is assigned by providing Young's modulus, E_c for balls and E_b for bonds, and the ratio of normal to shear stiffness, k_n/k_s and k_{nb}/k_{sb}. Other necessary bond properties include bond normal strength, σ_b, and bond shear strength, τ_b. The bond radius multiplier, λ, controls the diameter of the bond in reference to the smaller of the two bonded particles. Smaller bond radii result in higher bond stresses for the same displacement in shear or tension.

Table 6. PFC3D model micro-parameters

Particles	Bonds
$\rho = 1313$ kg/m^3	$\lambda = 1.0$
$(D_{max}/D_{min}) = 1.94$	$E_b = 4.48$ GPa
$E_c = 3.14$ GPa	$k_{nb}/k_{sb} = 1.62$
$k_n/k_s = 1.84$	$\sigma_b = 6.67 \pm 0.1$ MPa
$\mu = 0.49$	$\tau_b = 7.15 \pm 0.1$ Mpa

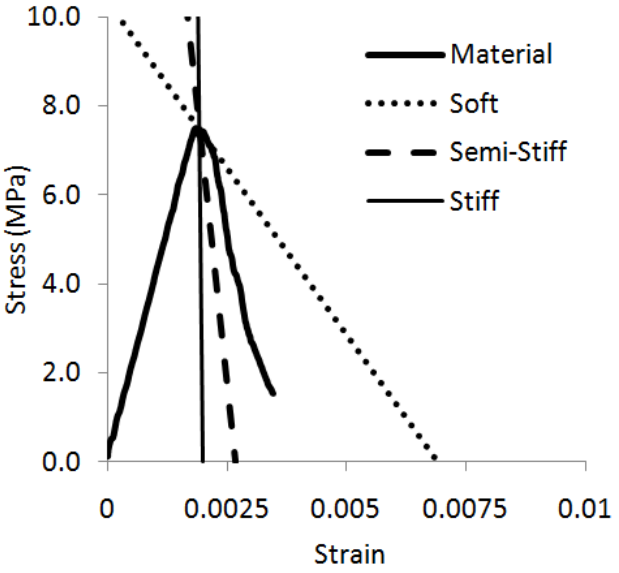

Fig. 17. Material response of PFC3D sample

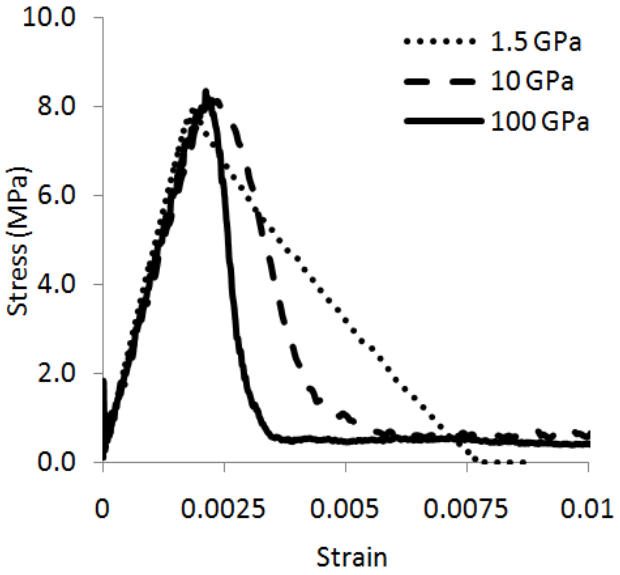

Fig. 18. PFC3D specimen response for varying platen stiffnesses

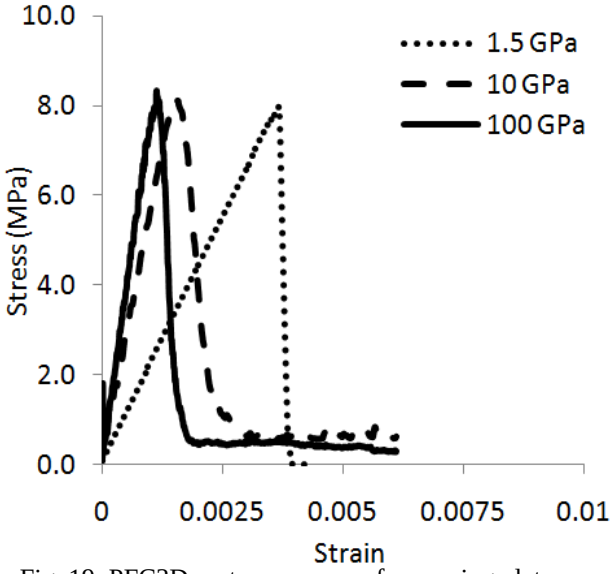

Fig. 19. PFC3D system response for varying platen stiffnesses

The model specimen is placed between a pair of infinitely strong elastic steel platens, also constructed from balls and bonds, having a specific elastic modulus and Poisson's ratio. The interface between the platens and the specimen is bonded with bonds of equal strength to those within the specimen. Three different tests were conducted by keeping the characteristic material same and varying the elastic modulus of the platens. Each test is loaded with a sufficiently slow strain rate to achieve a quasi-static loading condition. The 10 GPa and 100 GPa tests were run at a strain rate of 5% strain/second. To achieve a realistic platen rebound during unstable specimen failure, the 1.5 GPa test had to be run at 0.05% strain/second.

Fig. 17, Fig. 18, and Fig. 19 show the results from the UCS tests in PFC3D. Fig. 17 compares the material post peak behaviors obtained from different platen stiffness tests. The material curve was obtained from loading the specimen with constant displacement, which corresponds to a rigid loading condition. The soft system has a modulus of 1.5 GPa, the semi-stiff system has a modulus of 10 GPa, and the stiff system has a modulus of 100 GPa as compared to the targeted material post-peak modulus of -5.74 GPa.

Fig. 18 and Fig. 19 show the specimen and system stress-strain responses to loading. As in the case of FLAC3D and 3DEC, the plots show unstable failure for the soft (1.5 GPa) and stability for the stiff (100 GPa and 10 GPa) platens, where the specimen post-peak response follows platen rebound in the former and material characteristic curve in the latter. The residual strength in the graph is thought to be mostly due to particle interlocking occurring within the specimen.

Table 7 lists the post-peak modulus values obtained from the PFC3D model tests. These values are in agreement with the theory of unstable failure. Also, it conforms with the postulations set up in Fig. 3 and Fig. 4 that the specimen post-peak modulus should be similar to the platen modulus during unstable failure. Whereas in the stiff loading case, the specimen post-peak modulus is approximately the same as material pos-peak modulus.

Table 7. PFC3D test post-peak moduli

	Platen E (GPa)	Measured Specimen E_{pp} (GPa)	Specimen E_{pp} (GPa)
Soft	1.5	-1.35	-5.74
Semi-Stiff	10	-4.4	-5.74
Stiff	100	-10	-5.74

7. CONCLUSION

The study shows that the discrete element based numerical models FLAC3D and 3DEC can model stable and unstable rock failure through the use of a constitutive law with a softening component such as the strain softening model used in this study. The numerical model PFC3D is also shown to differentiate stable and unstable failures without needing a conventional constitutive law with a softening component. Onerous calibration processes are required for obtaining a desired stress-strain relationship for the material for all models but especially 3DEC and PFC3D.

REFERENCES

1. Itasca Consulting Group Inc. (2010) FLAC3D (Fast Lagrangian Analysis of Continua in 3 Dimensions), Version 4.0. Minneapolis, MN
2. Itasca Consulting Group Inc. (2010) 3DEC (3 Dimensional Distinct Element Code), Version 4.1. Minneapolis, MN.
3. Itasca Consulting Group Inc. (2010) PFC3D (Particle Flow Code in 3 Dimensions), Version 4.0. Minneapolis, MN.
4. Cook, N.G.W., (1965) A note on rockburst considered as a problem of instability. *Journal of the South African Institute of Mining and Metalurgy*, 437-46.
5. Wawersic, W.R. and Fairhurst, C. (1970) A study of brittle rock fracture in laboratory compression experiments. *International Journal of Rock Mechanics and Mining Science & Geomechanics Abstracts*, 7, 561-575.
6. Salamon, M., (1970) Stability, instability and design of pillar workings. *International Journal of Rock Mechanics and Mining Science & Geomechanics Abstracts*, 7(6), 613-631f.
7. Garvey, R. and Ozbay, U., 2011. Computer aided calibration of PFC3D coal samples using a genetic algorithm. *Proceedings of the 2nd FLAC/DEM Symposium*, Melbourne, Australia.